

June 2023

## Pathogen Emergence As Complex Biological Invasion: Lessons From Dynamical Systems Modeling

Sudam Surasinghe

*Yale University*, sudam.surasinghe@yale.edu

Marisabel Rodriguez

*Brown University*, mrodri85@asu.edu

Victor Meszaros

*Northeastern University*, v.meszaros@northeastern.edu

Jane Molofksy

*University of Vermont*, jane.molofksy@uvm.edu

Salvador Almagro-Moreno

*University of Central Florida*, samoreno@ucf.edu

*See next page for additional authors*

Follow this and additional works at: <https://orb.binghamton.edu/nejcs>



Part of the [Non-linear Dynamics Commons](#), [Numerical Analysis and Computation Commons](#), [Other Plant Sciences Commons](#), [Population Biology Commons](#), and the [Systems Biology Commons](#)

---

### Recommended Citation

Surasinghe, Sudam; Rodriguez, Marisabel; Meszaros, Victor; Molofksy, Jane; Almagro-Moreno, Salvador; and Ogbunugafor, Brandon (2023) "Pathogen Emergence As Complex Biological Invasion: Lessons From Dynamical Systems Modeling," *Northeast Journal of Complex Systems (NEJCS)*: Vol. 5 : No. 1 , Article 4. DOI: [10.22191/nejcs/vol5/iss1/4/](https://doi.org/10.22191/nejcs/vol5/iss1/4/)

Available at: <https://orb.binghamton.edu/nejcs/vol5/iss1/4>

This Article is brought to you for free and open access by The Open Repository @ Binghamton (The ORB). It has been accepted for inclusion in Northeast Journal of Complex Systems (NEJCS) by an authorized editor of The Open Repository @ Binghamton (The ORB). For more information, please contact [ORB@binghamton.edu](mailto:ORB@binghamton.edu).





---

# Pathogen Emergence As Complex Biological Invasion: Lessons From Dynamical Systems Modeling

## Authors

Sudam Surasinghe, Marisabel Rodriguez, Victor Meszaros, Jane Molofksy, Salvador Almagro-Moreno, and Brandon Ogbunugafor

## Pathogen Emergence As Complex Biological Invasion: Lessons From Dynamical Systems Modeling

Sudam Surasignhe<sup>1,2</sup>, Marisabel Rodriguez Messan<sup>3</sup>, Victor A. Meszaros<sup>1,3</sup>,  
Jane Molofsky<sup>4</sup>, Salvador Almagro-Moreno<sup>5</sup>, C. Brandon Ogbunugafor<sup>1,2,6,7,8</sup>

<sup>1</sup> Department of Ecology and Evolutionary Biology, Yale University, New Haven, CT, 06520 USA

<sup>2</sup> Public Health Modeling Unit, Yale School of Public Health, New Haven, CT 06510 USA

<sup>3</sup> Department of Ecology and Evolutionary Biology, Brown University, Providence RI, 02906 USA


<sup>4</sup> Department of Plant Biology, University of Vermont, Burlington, VT, 05405 USA


<sup>5</sup> Burnett School of Biomedical Sciences, University of Central Florida, Orlando, FL, 32816 USA

<sup>6</sup> Santa Fe Institute, Santa Fe, NM, 87501 USA

<sup>7</sup> Vermont Complex Systems Center, University of Vermont, Burlington, VT, 05405 USA

<sup>8</sup> Department of Chemistry, Massachusetts Institute of Technology, Cambridge, MA, 02139, USA

 The authors contributed equally to this work.

 Corresponding Author: brandon.ogbunu@yale.edu

### Abstract

Infectious disease emergence has become the target of cross-disciplinary efforts that aim to understand and predict the shape of outbreaks. The many challenges involved with the prediction of disease emergence events is a characteristic that infectious diseases share with biological invasions in many subfields of ecology (e.g., how certain plants are able to successfully invade a new niche). Like infectious diseases, biological invasions by plants and animals involve interactions between agents (pathogens and plants in their respective cases) and a recipient niche. In this study, we examine the problem of pathogen emergence through the lens of a framework first developed for the study of plant invasions, restructured to apply to pathogen invaders. We utilize mathematical techniques to examine how complex dynamics emerge between the various actors in a multi-component pathogen invasion process, which implies invasion frameworks can offer new insight on the particulars of infectious disease emergence. Summarizing, we consider these results in context of their application to epidemiology, and more broadly with regards

to modern efforts to bring the vernacular of complex systems to more real-world systems and problems. In doing so, we demonstrate the potential power in mathematizing conceptual models, and connecting ideas across disparate fields, toward a more rigorous picture of the nuances that underlie the dynamics of biological systems.

## 1 Introduction

Disease emergence, the process through which pathogens arise in a species and cause epidemics and pandemics, is one of the most important biological phenomenon of our time. Experts from across many intellectual and professional paradigms—ecology, evolutionary biology, epidemiology, economics, and others—have converged on this question, aiming to disentangle the many forces that underlie how a pathogen that is circulating in one species ends up causing a widespread epidemic in another.

Recent studies of disease emergence have contributed new perspectives about the macroecological influences [5], pathogen population genetics [6], molecular drivers [12], human behaviors [7] and myriad other forces that can drive emergence events [13]. The goal of these studies is to understand the underlying mechanics of emergence, and potentially predict outbreak events. However, prediction has proven to be a challenging feat in epidemiology for many reasons, including the manner in which the parameters that drive disease can change during the course of a pandemic [8]. Further, there is a growing body of literature that applies complex systems perspectives to public health [29].

Many models for biological invasion exist, some of which involve sequential steps or stages, from the introduction of an invader, to competition to native species in a new setting, to further propagation and spread [2, 9, 16, 17]. Other models have identified the drivers of microbial invasions, describing the interactions between alien and native microbial species [10], or developed conceptual models for epidemiological framings of invasion [27]. Despite the richness of this literature, few studies have attempted to integrate the study of disease emergence with general examinations of biological invasion using formal mathematical approaches. In particular, studies that incorporate multiple actors and stages of the invasion process.

In this study, we ask: can we animate qualitative models of biological invasion using tools of mathematical epidemiology? We propose that the grammar of disease emergence can be integrated with frameworks of biological invasions (e.g., from the plant invasion literature), and dynamical systems modeling to consider a stepwise, multi-component process through which an infectious pathogen (or an invading replicator of any kind) enters a new niche defined by a novel ecology (e.g., host biology). We find that mathematizing qualitative invasion frameworks can generate surprising and meaningful results that may speak to underappreciated complexity



in the pathogen emergence process. This includes co-existing equilibrium states between invading pathogen populations, and the importance of the carrying capacity of the invading population, which has implications for the success of an invader and its potential for equilibrium co-existence with a other standing (native) populations.

Summarizing, we discuss our results in terms of greater efforts to consider timely and important phenomena in biology and biomedicine as complex systems, with nonlinear interactions between actors and processes, and emergent patterns that contribute to the unpredictability of epidemics and pandemics.

## 2 Models & Methods: A Deterministic Model Of Invasion

### 2.1 Description

The following system models the population dynamics of a single invading pathogen population capable of establishment and spread within a host where-in another competing native population is present. This framework defines three unique states of invasion: *introduction*, *establishment*, and *spread*. The invading pathogen population transitions through each state as it competes with an already present native population. Below we elaborate on the characteristics of each invasive population state:

1. ***Introduction***: Defined as the state where-in the invading population is introduced into the novel host environment. This can occur through a number of ways: for example, a population of invading organisms can be brought into a new niche by "wind or wing" [18, 19]. Prior to introduction the invading population is completely external to the model system. Once introduced, invading population growth is modeled logistically. It is not guaranteed that the invading population transitions to the next invasive state. The invading population may not become established due to a myriad of factors including: failure to reproduce, in ability to utilize local resources, or predation.
2. ***Establishment***: Defined as the state where-in the invading population is able to persist within the host environment without the introduction of additional members of the invading population (from external to the system). Members of the invading population more suited to the novel host environment will have a higher probability of establishment.
3. ***Spread***: Defined as the stage where-in the invading pathogen population is both able to survive self-sustain in the host environment and reproduce. This allows the invading pathogen population to spread within the host environment and move further than its initial area of introduction. At this stage, the

invading population is considered invasive and undergoes competition with the native host population. Though not explicitly modeled in the system, upstream of this stage, the invading population disperses to new locations and can face additional pressure to establish in these new areas. [10].

## 2.2 Dynamical system for invasion

Let  $I(t)$ ,  $E(t)$ , and  $S(t)$  represent the invading pathogen population at each stage of the competition with a native species population  $N(t)$ . The rate of change of the invading pathogen population at introduction is defined as  $I'(t)$ . The invasion begins when the invading population, previously external to the model system, enters the novel host environment. The invading population is then said to be in the introduction state and we define its growth rate by the logistic growth function  $rI \left(1 - \frac{I}{K_I}\right)$ . Where  $r$  is the maximum per-capita growth rate of the invading population, and  $K_I$  is the maximum population density in the introduction state that host environment can sustain. The invading population can enter the novel host environment at a rate  $\beta I$ , with some probability of survival  $p$ . Here  $(1 - p)$  represents the probability the invading population is incapable of surviving, for example, due to not being able to reproduce. This portion of the invading pathogen population does not transition to the establishment stage.

The rate of change of the invading pathogen population at establishment is defined as  $E'(t)$ . The density of established members of the invading population increases as members are able to independently persist within the novel host environment. This is modeled via the terms  $p\beta I$ , where  $p$  is the probability of survival within the novel host environment. At this stage, the competitive pressure from the native host population is felt by the invading population. If the native host population is small the now established invading population has a higher probability of spreading. In order to model these competitive dynamics we take the product of an invasion rate, and the probability that members of the invading pathogen population will transition to the spread state  $\left(1 - \frac{N}{a+N}\right)$ . Here  $a$  is a half-saturation constant. Invading populations entering a novel host environment face sequential establishment risk [10]. In order to incorporate these dynamics into the model we assume the invading population can return to the establishment state at a rate  $\gamma$  to again compete with the native host population.

The rate of change of the invading pathogen population in the spread state is defined as  $S'(t)$ . At this stage the population has become self-sustaining, and its density increases as the population is able to reproduce and survive on its own without additional members necessarily needing to transition into the spread state. However, in the spread state the invading population continues to be subject to sequential establishment risk, if for example this self-reproducing segment is destabilized

be the native host population. While in the spread stage the invading population experience competitive pressure by the native host population. We incorporate these dynamics at this stage by a density dependent competition rate  $c_1N$ , where  $c_1$  defines the competitiveness of the native host population. At this stage, the invading population can die via a natural death rate of  $\mu_1$ .

The rate of change of the native host population within the system is defined as  $N'(t)$ . We model the growth rate of the native host population via logistic growth with a maximum per capita growth rate  $b$ , and a carrying capacity  $K_N$ . When the invading pathogen population is introduced into the native host environment we model native host competitiveness via competition coefficients  $c_2$  and  $c_3$ . The natural death of the native species is modeled via the constant linear term of  $\mu_2N$  with death rate  $\mu_2$ .

In summary, the dynamical system in equation (1) defines the deterministic model of invasion, and Figure (1) visualizes the behavior using the compartmental model.

$$\begin{aligned}
 I' &= \underbrace{rI \left(1 - \frac{I}{K_I}\right)}_{\text{Logistic growth rate}} - \underbrace{(1-p)\beta I}_{\text{Introduced into novel host environment \& incapable of survival}} - \underbrace{p\beta I}_{\text{Successful introduction \& survival}} \\
 E' &= \underbrace{p\beta I}_{\text{Successful introduction \& survival}} - \underbrace{\alpha E}_{\text{Transition rate}} \cdot \underbrace{\left(1 - \frac{N}{a+N}\right)}_{\text{Probability of spreading}} + \underbrace{\gamma S}_{\text{Sequential establishment risk}} \\
 S' &= \underbrace{\alpha E \left(1 - \frac{N}{a+N}\right)}_{\text{Successful transition rate}} - \underbrace{c_1NS}_{\text{Competition with native species}} - \underbrace{\gamma S}_{\text{Sequential establishment risk}} - \underbrace{\mu_1 S}_{\text{Natural death rate}} \\
 N' &= \underbrace{bN \left(1 - \frac{N + c_2S + c_3E}{K_N}\right)}_{\text{Native population growth rate as effected by competition with the invading population}} - \underbrace{\mu_2 N}_{\text{Natural death rate}}
 \end{aligned}
 \tag{1}$$

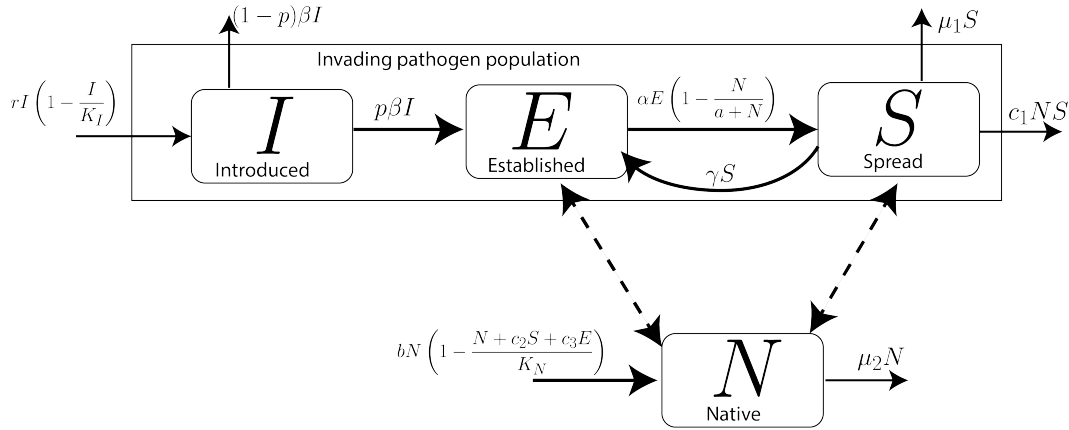


Figure 1: The compartmental diagram of the dynamical system (equation 1). This is an adaptation of a biological invasion model used to describe plant invasion [9].

### 2.3 Stability analysis

For simplicity, we assume  $\mu_1 = \mu_2 = 0$ , which leads to the system of ordinary differential equations (ODEs) represented in the equation (2).

$$\frac{dX}{dt} = \begin{bmatrix} \frac{dI}{dt} \\ \frac{dE}{dt} \\ \frac{dS}{dt} \\ \frac{dN}{dt} \end{bmatrix} = \begin{bmatrix} rI \left(1 - \frac{I}{K_I}\right) - \beta I \\ p\beta I - \alpha E \left(1 - \frac{N}{a+N}\right) + \gamma S \\ \alpha E \left(1 - \frac{N}{a+N}\right) - c_1 S N - \gamma S \\ bN \left(1 - \frac{N+c_2 S+c_3 E}{K_N}\right) \end{bmatrix} = F(X) \quad (2)$$

where,  $X = (I, E, S, N)$ . Furthermore, notice that  $I'$  only depends on  $I$ . Hence, the dynamic of the introduction phase is independent of the dynamics of the other populations. We will use the stability theory and Routh–Hurwitz stability criterion ([11]) to analyze the qualitative behavior of the model. The equilibrium solutions,  $X^*$  of the system of ODEs (equation (2)) are given by  $F(X^*) = 0$ , and

- $X_1^*(\theta) = (0, \theta, \frac{\alpha}{\gamma}\theta, 0), \theta \in \mathbb{R}^+ \cup 0$
- $X_2^* = (0, 0, 0, K_N)$
- $X_{3,4}^* = (I_{1,4}^*, E_{3,4}^*, S_{3,4}^*, N_{3,4}^*)$

are the major categories of fixed points. Here,  $I_1^* = \frac{(r-\beta)K_I}{r}$  and  $N_{3,4}^*$  can be determined as solutions to the equation (3), where

$$A_2 N^2 + A_1 N + A_0 = 0, \quad (3)$$

with coefficients defined as follows:

$$\begin{aligned} A_2 &= (ac_1\alpha + p\beta I_1^* c_1 c_3) > 0, \\ A_1 &= (p\beta I_1^* c_3 (ac_1 + \gamma) - ac_1\alpha K_N), \\ A_0 &= p\beta I_1^* a (c_2\alpha + c_3\gamma) > 0. \end{aligned}$$

Furthermore, the values of  $E_{3,4}^*$  and  $S_{3,4}^*$  are determined as follows:

$$E_{3,4}^* = \frac{p\beta I_1^* (c_1 N_{3,4}^* + \gamma)(a + N_{3,4}^*)}{ac_1 N_{3,4}^* \alpha} \text{ and } S_{3,4}^* = \frac{p\beta I_1^*}{c_1 N_{3,4}^*}.$$

Moreover, we use  $X_3^*$  and  $X_4^*$  to denote the fixed point corresponding to

$$N_3^* = \frac{-A_1 - \sqrt{A_1^2 - 4A_2A_0}}{2A_2} \text{ and } N_4^* = \frac{-A_1 + \sqrt{A_1^2 - 4A_2A_0}}{2A_2},$$

respectively.

**Remark (1).** For any positive parameter values, the  $X_1^*$  family of fixed points and  $X_2^*$  will exist.

**Remark (2).** Fixed points,  $X_{3,4}^*$  represent the co-existence of native and invasive species, which makes them interesting. However, the existence of these equilibria depend on the condition  $r > \beta$  and  $K_N \geq K_N^*$ . To achieve those equilibria, the carrying capacity must be greater than a critical value which depends on other parameters.

If  $I^*$  and  $N^*$  strictly positive then by analysing the discriminant of equation (3), critical carrying capacity is given by,

$$K_N^* = \frac{p\beta I_1^* c_3 (ac_1 + \gamma) + 2\sqrt{A_2A_0}}{ac_1\alpha}. \quad (4)$$

Furthermore,  $X_3^*$ ,  $X_4^*$  both present when  $K_N > K_N^*$  and  $X_3^* = X_4^*$  when  $K_N = K_N^*$ . However, there is no co-existed population when  $K_N < K_N^*$ . (Visual illustration is provided in the supplementary figure S1.)

The stability analysis can be discussed using the linearized system. The eigenvalues  $\lambda$  of the Jacobian matrix  $J(X^*)$  (see supplemental document equation 10) of the system for a fixed point  $X^* = (I^*, E^*, S^*, N^*)$  is given by the characteristic polynomial of the form,

$$\left( r \left( 1 - \frac{2I^*}{K_I} \right) - \beta - \lambda \right) (\lambda^3 + B_2\lambda^2 + B_1\lambda + B_0) = 0 \quad (5)$$

where  $B_i$ ,  $i = 0, 1, 2$  will depends on  $X^*$  and parameter values (check supplemental document equation 11 for detail explanation). Hence, the first eigenvalue of the Jacobian matrix  $J(X^*)$  is determined as  $\lambda_1 = r \left(1 - \frac{2I^*}{K_I}\right) - \beta$ , while the remaining eigenvalues satisfy the cubic polynomial equation

$$\lambda^3 + B_2\lambda^2 + B_1\lambda + B_0 = 0 \tag{6}$$

The Routh-Hurwitz criterion [11] can be used to determine whether the eigenvalues of a linearized system at the fixed point  $X^*$  are located in the left half-plane. When applied to third-order polynomials (equation 6), the criterion requires that  $B_1$ ,  $B_2$  and  $B_3$  are positive and  $B_2B_1 > B_0$ . Table (1) summarizes the existence and local stability of each fixed point.

- *Local Stability of  $X_1^*$* : Let's consider  $J(X_1^*)$  and observe that the characteristic polynomial can be expressed as follows:

$$(\lambda - (r - \beta))\lambda(\lambda - b\left(1 - \frac{c_2S^* + c_3E^*}{K_N}\right))(\lambda + (\alpha + \gamma)) = 0.$$

This polynomial is obtained by substituting  $I^* = 0$  and  $N^* = 0$  into the equation (5). Therefore, eigenvalues for  $J(X_1^*)$  are given by  $\lambda_1 = (r - \beta)$ ,  $\lambda_2 = 0$ ,  $\lambda_3 = b\left(1 - \frac{c_2S^* + c_3E^*}{K_N}\right)$  and  $\lambda_4 = -(\alpha + \gamma)$ . Since it has an eigenvalue of zero, the system is not locally asymptotically stable at  $X_1^*$ .

- *Local Stability of  $X_2^*$* : The eigenvalues of  $J(X_2^*)$  are given by  $\lambda = (r - \beta)$  and the roots of equation (6), where  $B_2 = b + D_1 + D_2$ ,  $B_1 = b(D_1 + D_2) + D_1c_1K_N$  and  $B_0 = bD_1c_1K_N$ . Here,  $D_1 = \frac{\alpha a}{a + K_N}$  and  $D_2 = \frac{\alpha a}{a + K_N}$ . It is worth noting that these eigenvalues satisfy the Routh-Hurwitz criterion since  $B_1$ ,  $B_2$  and  $B_3$  are positive (an assumption already met, given that parameters are positive) and  $B_2B_1 > B_0$  (as shown in equation 7).

$$\begin{aligned} B_2B_1 - B_0 &= (b + D_1 + D_2)(b(D_1 + D_2) + D_1c_1K_N) - bD_1c_1K_N \\ &= b^2(D_1 + D_2) + b(D_1 + D_2)^2 > 0. \end{aligned} \tag{7}$$

Hence, the eigenvalues corresponding to equation 6 (for the fixed point  $X_2^*$ ) possess a negative real part. Therefore,  $X_2^*$  is locally asymptotically stable if and only if  $r < \beta$ .

- *Local Stability of  $X_{3,4}^*$* : When  $I^* = I_1^*$ , the first eigenvalue  $\lambda = -(r - \beta)$  and  $X_{3,4}^*$  is unstable if  $r < \beta$ . Furthermore, if  $r > \beta$  then the first eigenvalue is negative and we can use the Routh-Hurwitz stability criterion for equation (6)

to determine whether the real part of each eigenvalue is negative. In this case,  $B_0$  at  $N_{3,4}^*$  is denoted by  $B_0(N_{3,4}^*)$  and can be expressed as

$$B_0(N_{3,4}^*) = \frac{bA_2}{K_N(a + N_{3,4}^*)} \left( N_{3,4}^2 - \frac{A_0}{A_2} \right),$$

where  $A_2, A_1$ , and  $A_0$  are the coefficients of equation (3). It is important to note that  $\frac{bA_2}{K_N(a+N_{3,4}^*)} > 0$  (with the assumption  $N > 0$ ) and

$$N_3^* \leq \sqrt{\frac{A_0}{A_2}} = \frac{-A_1}{2A_2} = N_{3,4}^*(K_N^*),$$

where  $N_{3,4}^*(K_N^*)$  denotes the  $N_{3,4}^*$  value at  $K_N^*$ . Therefore,  $B_0(N_3^*) < 0$  for any  $K_N \geq K_N^*$ , which violates the Routh-Hurwitz criterion. Hence,  $X_3^*$  is an unstable fixed point.

Since  $N_4^* > \sqrt{\frac{A_0}{A_2}}$ , we have  $B_0(N_4^*) > 0$ . Moreover,  $B_2$  is positive for any positive  $N$ . Therefore, to determine the stability of  $N_4^*$ , we need to satisfy only one condition. Specifically,  $N_4^*$  is locally asymptotically stable if and only if  $B_1 > \frac{B_0}{B_2}$ . In the subsequent section, we will further analyze the local stability of  $X_4^*$  using numerical methods.

Equilibrium	Existence	Stability
$X_1^*(\theta) = (0, \theta, \frac{\alpha}{\gamma}\theta, 0)$	Always	Always unstable (at least one eigenvalue is zero)
$X_2^* = (0, 0, 0, K_N)$	Always	LAS if and only if $r < \beta$ , otherwise it is unstable.
$X_{3,4}^* = (I_1^*, E_{3,4}^*, S_{3,4}^*, N_{3,4}^*)$	$r > \beta$ and $X_3^* = X_4^*$ when $K_N = K_N^*$ or $X_3^* \neq X_4^*$ when $K_N > K_N^*$	If $N_{3,4}^*$ exists and is positive, <ul style="list-style-type: none"> <li>• <math>X_3^*</math> is always unstable.</li> <li>• <math>X_4^*</math> LAS if and only if <math>B_1 &gt; \frac{B_0}{B_2}</math>.</li> </ul>

Table 1: Summary of boundary and interior equilibrium dynamics. LAS: locally asymptotically stable.

### 3 Results

In this section, we investigate the long-term behavior of the populations by employing a numerical ordinary differential equation (ODE) solver, specifically the

MATLAB-ode45 solver. The MATLAB-ode45 solver utilizes an explicit Runge-Kutta (4,5) formula and employs a variable step size and adaptive algorithm to adjust the step size accordingly [20, 21]. For our simulations, we utilize the default settings of the MATLAB-ode45 solver. The tolerance levels are set to a relative tolerance of  $10^{-3}$  and an absolute tolerance of  $10^{-6}$ . The maximum step size is set to 0.2. The simulations are conducted over a time interval of  $[0, 1000]$  or until the results become unbounded.

The compartment model utilized in this study has a sequential structure that leads to an independent introduction population, where  $I'$  is a function of only  $I$ . Additionally, note that the introduction population follows a logistic growth model with removal, as illustrated in Figure (S2A). Hence, as  $t \rightarrow \infty$ , we have

$$I^* = \begin{cases} 0, & \text{if } r \leq \beta : \text{Failed Introduction} \\ I_1^* = \frac{(r-\beta)K_I}{r}, & \text{if } r > \beta : \text{Successful Introduction} \end{cases} \quad (8)$$

For the qualitative analysis of the model, we can reduce the system to a 3D model and replace the term  $p\beta I = p\beta I^*$  in the  $E'$  equation. Furthermore, the change in the total invasive population, in the long run (note that  $I \rightarrow I^*$  in the long run), can be described by the following equation:

$$\frac{dM}{dt} = \frac{dI}{dt} + \frac{dE}{dt} + \frac{dS}{dt} = p\beta I^* - c_1 NS, \quad (9)$$

where  $M = I + E + S$  is the total invasive population. In the following two subsections, we will examine scenarios for both failed and successful introduction of the invasive population. For a summary of these scenarios, refer to figure (11).

### 3.1 Failed Introduction of the Invasive population

When the removal rate ( $\beta$ ) from the introduction compartment exceeds the growth rate ( $r$ ), the introduction invasive population will die out ( $I^* = 0$ ). This can result in one of two outcomes ( $X_2^*$  or  $X_1^*(\theta)$ ).

If there is a native attacking population ( $N > 0$ ), the invasion will fail, and the invasive population ( $I, E, S$ ) will disappear as  $\frac{dM}{dt} = -c_1 NS < 0$ . As illustrated in Figure (S2B), the native population will eventually reach its carrying capacity ( $K_N$ ).

If there is no native attacking population ( $N = 0$ ), the total invasive population will remain constant ( $M(t) = M(t_0)$  for  $t \geq t_0$ , where  $t_0$  is the initial time), as  $\frac{dM}{dt} = 0$ . In this case, a center manifold can be observed in the  $ES$  plane, as shown in Figure (2). Every point in the  $ES$  space is attracted to a fixed point  $S^* = \frac{\alpha}{\gamma} E^*$  for some  $E^* \geq 0$ . This indicates that the invasion will succeed with an initially



positive established population, in which some invaders survive and establish before the introduced population dies out.

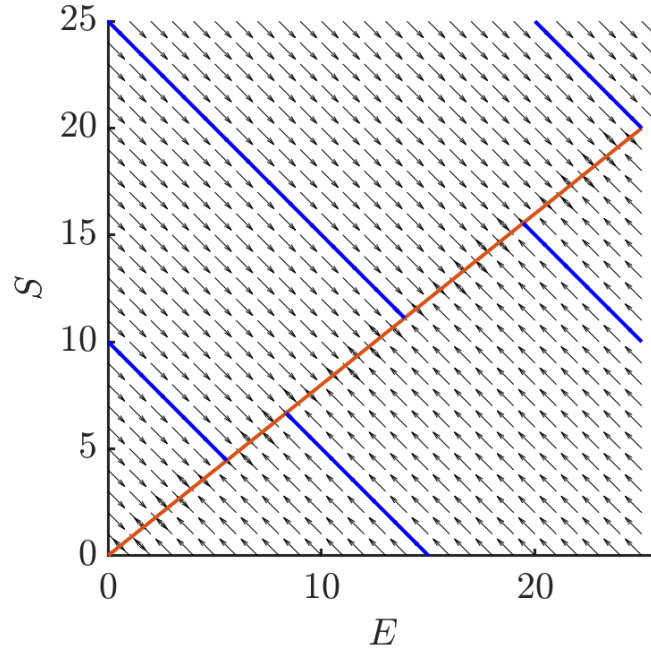


Figure 2: Dynamics of the established ( $E(t)$ ) and Spread ( $S(t)$ ) population with  $I(0) = 0, N(0) = 0$ . This figure demonstrates that each point in  $ES$  plain will attract a fixed point  $S^* = \frac{\alpha}{\gamma}E^*$  for some  $E^* > 0$ . Each point in the red line is a fixed point of the system and blue curves are trajectories that approach different fixed points in the red curve. This suggests that for some parameter values, the established and spread populations can converge to different equilibrium values depending on the starting point.

An intriguing and non-trivial scenario arises when the introduction of the invasive population is successful, which occurs when the growth rate ( $r$ ) is greater than the removal rate ( $\beta$ ). In the following analysis, we assume  $r > \beta$ .

### 3.2 Extinction of the Native replicator population

This scenario occurs when the carrying capacity of the Native population is relatively low. Specifically, if there exists a carrying capacity value  $K_N = K_N^1$  such that  $K_N^1 < N(t) + c_2S(t) + c_3E(t)$  for all  $t$  within the interval  $(t_0, T)$ , where  $T$  is a finite time, and if the native population reaches extinction ( $N(T_0) = 0$ ) at some time  $T_0$  within the interval  $(t_0, T]$ , then it follows that the derivative of the native population, denoted as  $N'$ , is negative in the time interval  $(t_0, T)$ . In other words, the Native

population will continuously decrease over time within this interval. Furthermore, since the native population size  $N$  is equal to 0 at a certain time  $T_0$  within the interval  $(t_0, T]$ , it follows that the native population remains at 0 for all times  $t$  greater than or equal to  $T_0$ . In other words, once the Native population reaches extinction ( $N = 0$ ) at  $T_0$ , it remains extinct thereafter. It should be noted that for any carrying capacity value  $K_N$  smaller than  $K_N^1$ , a similar behavior can be observed. Therefore, if such a scenario exists where the native population reaches extinction, the maximum carrying capacity value that leads to the extinction of the native population is denoted as  $K_N^1$ . In other words,  $K_N^1$  represents the largest carrying capacity for which the native population can become extinct.

In situations where there is no native population, or the native population dies out, the successful introduction of the invasive population ( $I \rightarrow I_1^*$  as  $t \rightarrow \infty$ ) results in an exponential growth of the invasive population. Our model explains this phenomenon through the equation  $\frac{dM}{dt} = p\beta I_1^* > 0$ . Figure (3) depicts the dynamics of the established and spread population in this scenario. The invasive population will continue to grow without limit. This result is in agreement with previous studies on invasive species and highlights the importance of preventing the introduction of invasive species to new environments to avoid ecological damage [24, 25].

In this study, we have observed that the  $K_N < K_N^*$  leads to the extinction of the native population. Specifically, if  $K_N$  is less than  $K_N^*$ , there are no solutions to the equations  $K_N - (N + c_2S + c_3E) = 0$  and  $K_N < N + c_2S + c_3E$  for any positive initial values of  $N$ ,  $E$ , and  $S$ . Consequently, the native population decreases over time and eventually becomes extinct, while the invasion of the invasive population succeeds.

To further investigate and determine an upper bound for this case, we have conducted a numerical analysis of the parameters  $K_N$  and  $K_I$ , while keeping all other parameters fixed. We consider a specific set of parameter values represented as a vector  $\Psi$  for reference, denoted by  $\Psi = (p = 0.8, \beta = 0.5, \alpha = 0.3, a = 0.8, \gamma = 0.5, b = 4, c_1 = 0.3, c_2 = 0.4, c_3 = 0.1, r = 3)$ . These parameter values have been chosen to facilitate the demonstration of our analysis results.

In the plot shown in figure (6), the black curve represents the values of  $K_N^1$  for different values of  $K_I$ . This curve serves as a threshold, indicating that for any given carrying capacity of the invasive population ( $K_I$ ), if the carrying capacity of the native population ( $K_N$ ) is below the corresponding value on the black curve ( $K_N^1$ ), the invasive population will undergo exponential growth while the native population gradually diminishes and eventually becomes extinct. This observation emphasizes the crucial role of the carrying capacity of the native population in determining the outcome of the invasion process.

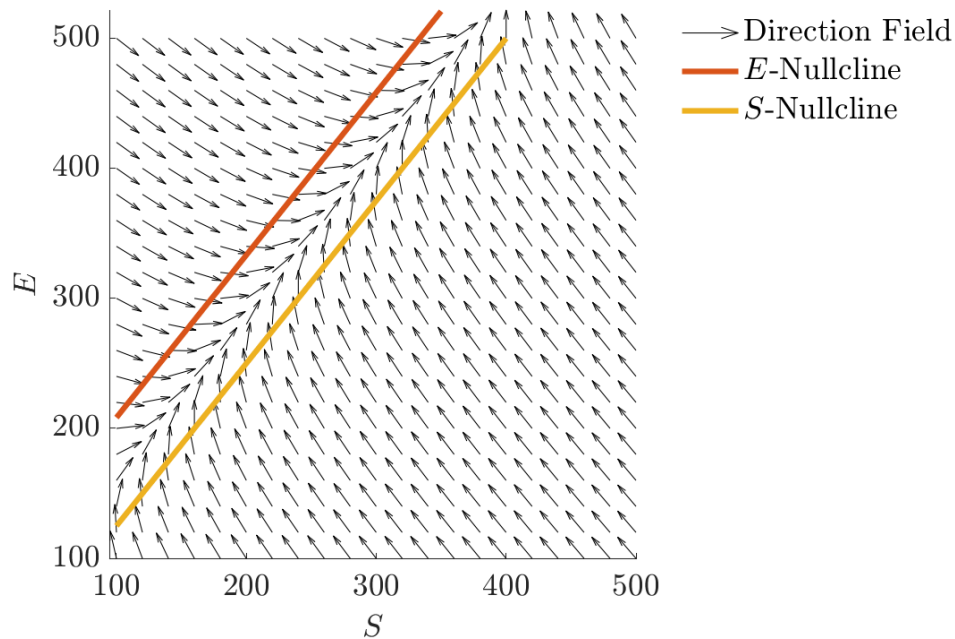


Figure 3: Long-term dynamics of invasion in the case of native extinction. In the situation where the native population becomes extinct ( $N \rightarrow 0$ ) and the introduction of invasion is successful ( $I \rightarrow I_1^*$ ) in the long run, the dynamics of the established and spread population will be trapped within the region defined by the parallel lines that correspond to the  $E$  and  $S$  nullclines.

### 3.3 Co-existing Native and Invasive populations:

The coexistence of native and invasive populations can occur when we have a successful introduction of the invasive species and the non-extinction of the native species. This condition is possible when the maximum growth rate of the invasive species ( $r$ ) is greater than its introduction rate ( $\beta$ ), and the carrying capacity of the native species ( $K_N$ ) is larger or equal to the critical value ( $K_N^1$ ) explained in the section (3.2). In other words, in order to observe the coexistence of native and invasive species, it is essential for the invasive species to have a higher growth potential during the introduction phase and for the native species to have a sufficient carrying capacity.

Due to the dependence of critical values such as  $K_N^*$  on parameters such as  $p$ ,  $r$ ,  $\beta$ , and  $K_I$ , we have deemed it necessary to conduct a more in-depth analysis to explore the sensitivity of the parameters  $K_N$  and  $K_I$ . We conducted a numerical study to explore the sensitivity of the carrying capacities  $K_N$  and  $K_I$ , while keeping

all other parameters fixed. The results of our study were obtained using a set of fixed parameter values denoted as a vector,  $\Psi$ . Specifically, we used the following parameter values for reference:  $\Psi = (p = 0.8, \beta = 0.5, \alpha = 0.3, a = 0.8, \gamma = 0.5, b = 4, c_1 = 0.3, c_2 = 0.4, c_3 = 0.1, r = 3)$ . These parameter values were chosen to be consistent across our study, allowing us to demonstrate and interpret the numerical results accurately. By systematically varying the values of  $K_N$  and  $K_I$ , we examined the dynamics of the coexisting populations. This analysis allowed us to identify the range of carrying capacity values for both native and invasive species that lead to their stable coexistence. By studying the effects of different parameter combinations, we gained insights into the conditions necessary for the long-term coexistence of these species.

#### *Stability of co-existing fixed points ( $X_{3,4}^*$ )*

The stability analysis of the co-existing fixed points ( $X_{3,4}^*$ ) is conducted by numerically evaluating the eigenvalues of the Jacobian matrix at these fixed points. This analysis is performed for a given set of parameters, and the sign of the maximum real part of the eigenvalues is examined. The results of this numerical evaluation, considering parameter values  $\Psi$  and  $(K_I, K_N) \in [0, 200]^2$ , are presented in Figure (4). The depicted figure confirms the previous qualitative analysis presented in Section (2.3), showing that the fixed point  $X_3^*$  is always unstable. It is noteworthy that the critical value  $K_N^*$  represents a limit point bifurcation point with respect to the parameter  $K_N$ , as  $X_{3,4}^*$  fixed points disappear when  $K_N < K_N^*$ . Additionally, the figure reveals the critical values of the carrying capacity for the fixed point  $X_4^*$  to be locally asymptotically stable. These critical values indicate the occurrence of bifurcation points.

#### *Bifurcation analysis for $K_N$ and $K_I$*

Bifurcation analysis is performed to study the qualitative changes [32,34] in the dynamics of the system (equation (2)) as parameters  $K_N$  and  $K_I$  vary. To numerically estimate the bifurcation points for the given values of  $K_N$  and  $K_I$ , we utilize the MatCont package [26] in MATLAB (with ODE45 solver). Figure (5B) presents the bifurcation diagram illustrating the behavior of the system for different values of  $K_N$  for fixed  $K_I = 100$  and  $\Psi$  parameters. As discussed in the previous section, the diagram clearly demonstrates the presence of a limit point bifurcation [26] at the critical value  $K_N^*$ . This bifurcation marks the boundary where the fixed points  $X_{3,4}^*$  cease to exist as  $K_N$  decreases below  $K_N^*$ . Similar behavior occurs as  $K_I$  increases for given parameters  $K_N = 125$  and  $\Psi$ . As  $K_I$  increases, the bifurcation diagram (figure (5A)) exhibits similar patterns, showcasing the influence of  $K_I$  on

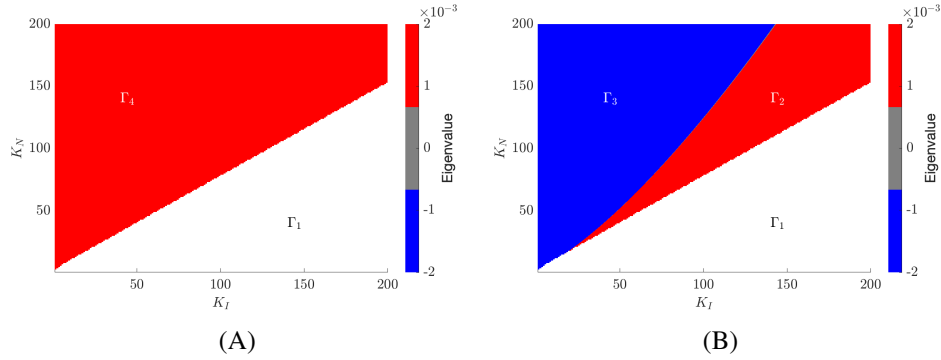


Figure 4: Stability of the fixed points. This figure demonstrates An illustration of the variations in the stability of the fixed points (A)  $X_3^*$  and (B)  $X_4^*$  in relation to the parameters  $\Psi$  and  $(K_I, K_N) \in [0, 200]^2$ . The plot represents the sign of the maximum real part of the eigenvalues obtained from the Jacobian matrix at each fixed point. In the white region ( $\Gamma_1$ ), the fixed point does not exist. In the red region ( $\Gamma_4$  for (A) and  $\Gamma_2$  for (B)), at least one of the eigenvalues has a positive real part, indicating instability. Conversely, in the blue region ( $\Gamma_3$ ), the real parts of all eigenvalues are negative, indicating stability.

the system dynamics.

Moreover, the presented bifurcation diagrams (Figure (5)) provide insights into the existence of a Hopf bifurcation, more precisely an Andronov-Hopf bifurcation [26], in relation to the parameter values  $K_N$  and  $K_I$ , while keeping the remaining parameters  $\Psi$  fixed. This bifurcation indicates the emergence of periodic solutions or limit cycles [35, 36] in the system dynamics. To refer to the critical value of  $K_N$  associated with the Hopf bifurcation, we denote it as  $K_N^{(2)}$  for further discussion and analysis.

### Periodic orbit

As explained in the previous section, the emergence of a periodic orbit can be attributed to the presence of Hopf bifurcation points [35, 36]. Figure (6) illustrates the locations of limit point bifurcation and Hopf bifurcation points in the  $K_I, K_N$  parameter space with fixed parameters  $\Psi$ . The values  $K_N^*$  and  $K_N^{(2)}$  are functions of  $K_I$ . Additionally, it should be noted that the coexisting fixed point  $X_4^*$  becomes unstable within specific regions of parameter values  $(K_I, K_N)$ , which are bounded by the curves  $K_N^{(2)}$  and  $K_N^*$ . Therefore, these supercritical Hopf bifurcation points ( $K_N^{(2)}$ ) indicate the emergence of a locally asymptotically stable limit cycle [33, 35, 36] around the unstable fixed point  $X_4^*$ . Figure (7A) illustrates the dynamics of the system, specifically stable periodic orbits, when the carrying capacity of the native

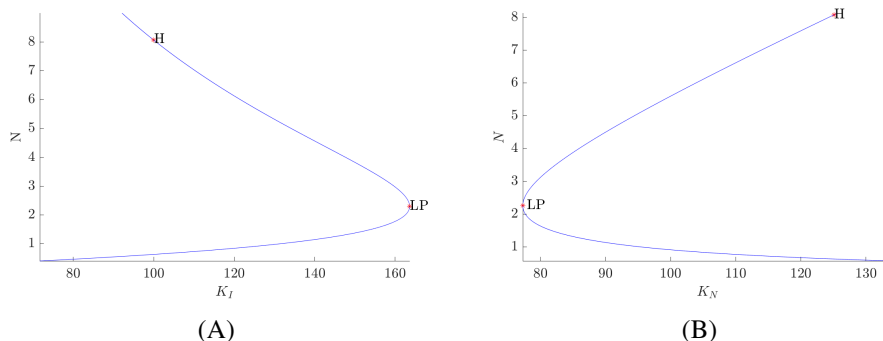


Figure 5: Bifurcation analysis for  $K_I$  and  $K_N$ . This figure demonstrates the bifurcation points for (A)  $K_I$  with  $K_N = 125$  and (B)  $K_N$  with  $K_I = 100$ , while keeping the other parameters fixed at  $\Psi$ . The plot shows the occurrence of both Limit Point(LP) bifurcation and Hopf bifurcation points for these parameters. It is evident that there is an interdependence between the effects of  $K_I$  and  $K_N$ , indicating the complex relationship between the two parameters in determining the system dynamics.

population is slightly less than  $K_N^{(2)}$  while keeping  $K_I$  fixed at 100 and using the parameter set  $\Psi$ .

As discussed in Section (3.2), when the carrying capacity of the native population ( $K_N$ ) is below the critical value  $K_N^1$ , the native population becomes extinct. In the case where  $K_N$  is already below the critical value  $K_N^{(2)}$ , a decrease in  $K_N$  (while keeping  $K_I$  fixed) leads to an increase in the amplitude of the periodic solution  $N(t; K_N)$ . It is important to note that the minimum value of the periodic solution  $N(t; K_N)$  decreases in this scenario (as  $K_N < K_N^{(2)}$  decrease), and it reaches zero when  $K_N$  equals  $K_N^1$ . In Figure (6), the black curve represents the values of  $K_N^1$  for the fixed parameter set  $\Psi$ . This curve indicates the critical threshold for the carrying capacity of the native population below which the native population becomes extinct. The  $K_N^1$  values provide insight into the parameter range where the native population cannot survive in the presence of the invasive species. Therefore, in the parameter space of  $K_I$  and  $K_N$  (with the fixed parameter set  $\Psi$ ), a stable limit cycle will be present in the system when the parameter values fall within the region bounded by the  $K_N^1$  and  $K_N^{(2)}$  curves, as shown in Figure (6). This region represents the parameter range where the native population coexists with the invasive species, exhibiting periodic oscillations. Figure (7B) demonstrates the change in the dynamics around the critical  $K_N^1$  with  $K_I = 100$  and  $\Psi$ .

*Example: Dynamics of the system when  $K_I = 100$  with parameter set  $\Psi$*

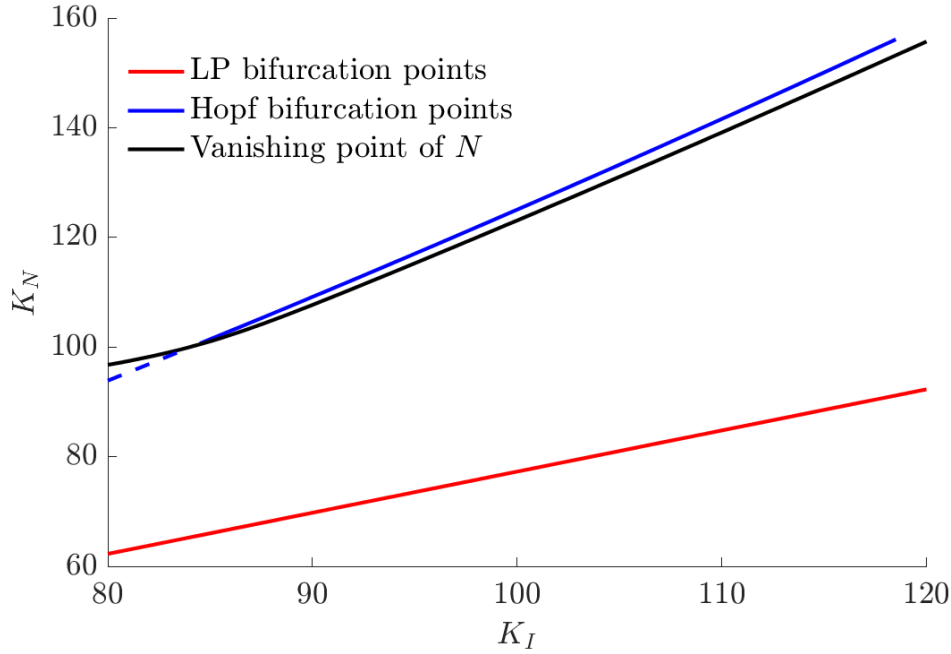


Figure 6: Bifurcation points for  $(K_I, K_N)$ . The figure showcases the bifurcation points in the parameter space  $(K_I, K_N)$  with the fixed parameter set  $\Psi$ . It highlights three key points: the Limit Point (LP) bifurcation points denoted as  $K_N^*(K_I)$ , the Hopf bifurcation points denoted as  $K_N^{(2)}(K_I)$ , and the points denoted as  $K_N^1(K_I)$  that determine the extinction of the native population. The plot provides valuable information about the system’s behavior based on different ranges of  $K_N$  and  $K_I$  values. Specifically, if  $K_N \leq K_N^1$ , the invasive population will grow exponentially, leading to the extinction of the native population. If  $K_N^1 < K_N < K_N^{(2)}$ , the system exhibits a stable periodic co-existing solution. Finally, if  $K_N > K_N^{(2)}$ , the system reaches a stable co-existing fixed point.

To illustrate the dynamics of the system, we have chosen an example with  $K_I = 100$  and the parameter set  $\Psi$ . We observe that with the given parameter values, the critical carrying capacity  $K_N^*$  is approximately 77.31. It is important to note that in the absence of the native population ( $N(t) = 0$  for  $t > T_0$ , where  $T_0$  is a finite time), the invasive population ( $E(t)$  and  $S(t)$ ) grows exponentially, as shown in Figure (8). To prevent the extinction of the native population, we numerically calculate the critical carrying capacity for this example, which is approximately  $K_N^1 \approx 123.129$ , as depicted in Figure (7B). This value represents the threshold beyond which the native population can persist in the presence of the invasive species. The presence of the limit cycle is observed in the range of  $(K_N^1, K_N^{(2)})$  for the carrying capacity  $K_N$ . This range represents the critical values of  $K_N$  where the system

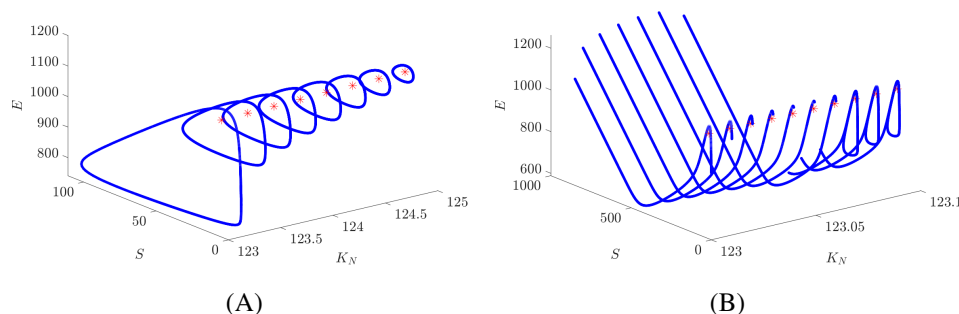


Figure 7: The sensitivity of the system to variations in the carrying capacity of the native population. This figure displays the behavior of the system as  $K_N$  varies around critical values, while keeping  $K_I$  fixed at 100 and other parameters set to  $\Psi$ . Plot (A), demonstrates the presence of a stable periodic orbit in the region of  $123.13 < K_N < 125.01$ . This indicates the coexistence of the native and invasive populations in a cyclic pattern. On the other hand, plot (B) illustrates the change in dynamics around the specific value of  $K_N = 123.1$ , where the native population becomes extinct.

exhibits stable oscillations and coexistence of the native and invasive species. Furthermore, we find that the fixed point  $X_4^*$  becomes stable after the critical carrying capacity  $K_N^{(2)}$ , which is approximately 125.02 for this example. All these scenarios are demonstrated in figure (8), which shows the change in the dynamics of  $E$  and  $N$  with the parameter  $K_N$ . The native population initially attempts to reach its carrying capacity. However, due to the presence of invasive species, they will either die out or decline to a lower value.

*Stable periodic orbit:* As illustrated in Figure (7A), when the carrying capacity of the native population  $K_N$  falls within the range  $(K_N^1, K_N^{(2)}) \approx (123.13, 125.01)$ , the system exhibits a stable limit cycle. This means that the population dynamics of both the native and invasive species oscillate periodically over time, indicating the coexistence of the two species in a stable manner. By choosing  $K_N = 124$ ,  $K_I = 100$ , and the parameter set  $\Psi$ , we can illustrate the stable periodic orbit of the system. The figure (9) demonstrates the trajectories  $X(t)$  with initial conditions  $(1, 1060, 10, 20)$ , and  $(1060, 13.94, 12, 250/3)$  are approaching ( $t \in [0, 10000]$ ) to a periodic orbit. Furthermore, we investigate the  $X(t)$  trajectory with initial condition  $(1, 1060, 10, 20)$  in projected spaces and demonstrate the behavior of the system by time series data. Figure (10) (and S3)) visualize the dynamics of the system for the parameter  $\Psi$  and  $K = 124$  with initial condition  $(1, 1060, 10, 20)$ . Additional figures which illustrate the dynamics of the system can be found in the supplemental document.



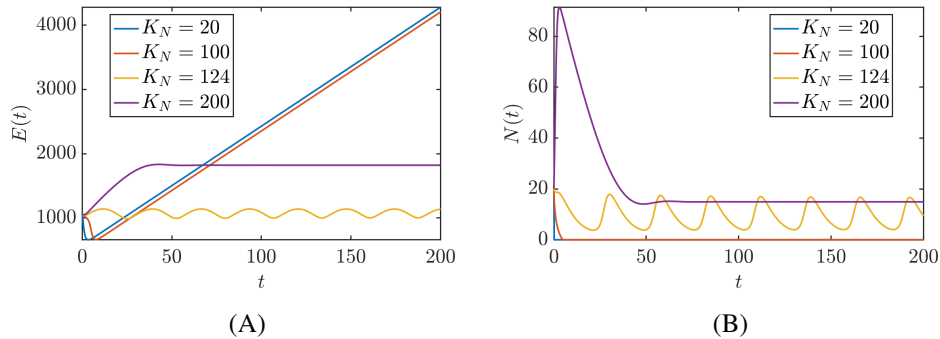


Figure 8: Sensitivity Analysis. This shows the sensitivity analysis of parameter  $K_N$ . It demonstrates the changes in dynamics of (A) established and (B) native populations with carrying capacity  $K_N$ . This reveals how the system of biological invasion is highly sensitive to the carrying capacity of the native compartment. (The initial condition [1060 10 20 1] is used to carry out the computation.)

After conducting both analytical and numerical analysis of the system dynamics, the results can be summarized (see Figure (11)) into two main cases: failed and successful introduction. In the case of a failed introduction, the native population reaches its carrying capacity while the invasive population dies out, resulting in a trivial scenario. On the other hand, a successful introduction leads to a successful invasion, with three possible end scenarios determined by the carrying capacity of the native population. If the carrying capacity is relatively low, the native population will eventually go extinct while the invasive population grows exponentially. If the carrying capacity is relatively high, the system exhibits a coexisting stable equilibrium, where both populations can coexist in the long term. The third possibility occurs when the carrying capacity is in the intermediate range, resulting in coexisting periodic behavior between the native and invasive populations.

### *Agent-based model*

In the Supplementary Material, we have provided an agent-based modeling (ABM) approach, that can be examined for those interested methods that allow for the modeling of discrete states, actors, and time steps [4, 14]. In this study, the agent-based approaches are stochastic in nature, where each agent's next condition is weighted by a random probability at each timestep. We emphasize, however, that the mathematical approaches are the basis for the arguments and conclusions, with the ABM serving a supporting role. Nonetheless, it can be useful to explore other approaches for questions around complex biological systems. A more rigorous dual-approach might be useful, but is beyond the scope of this manuscript, as

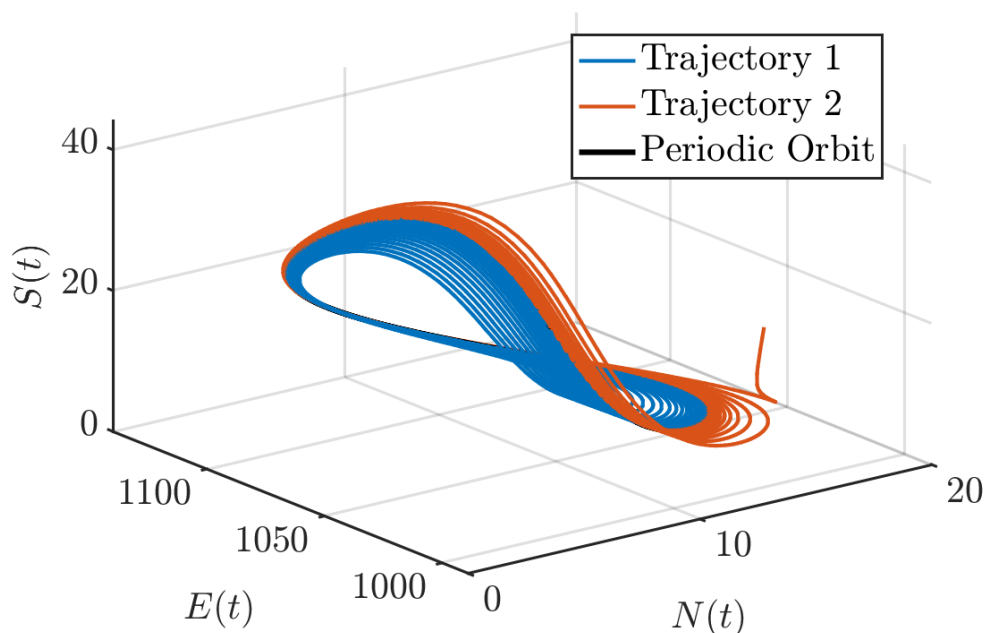


Figure 9: The figure demonstrates the trajectories  $X(t)$  started with initial conditions (IC)  $(250/3, 1060, 13.94, 12)$ , and  $(1, 1060, 10, 20)$  are approaching to a periodic orbit. Here  $t \in [0, 10000]$ ,  $K_N = 124$  and other parameter values are from  $\Psi$ .

the mathematical results are substantive.

## Discussion

In this study, we applied concepts derived from a qualitative model of biological invasion towards the problem of infectious disease emergence. In order to transcend these past descriptive summaries, we employ mathematical methods that include compartmental models, which are standard in the study of epidemics. These methods offer many benefits, and are especially resonant with models of biological invasion because they offer discrete populations that are synonymous with discrete decision points along the invasion trajectory that can allow one to design more effective disease control strategies. More specifically, we utilize ordinary differential equations approaches, as they are standard in studying epidemiological phenomena, and are effective in tracking the dynamics of populations, using continuous state variables, and analytical, transparent descriptions of populations.

Disease emergence has been described in terms of a complex systems approaches [3, 28, 29]. Our study applies a conceptual model of biological invasion to the prob-

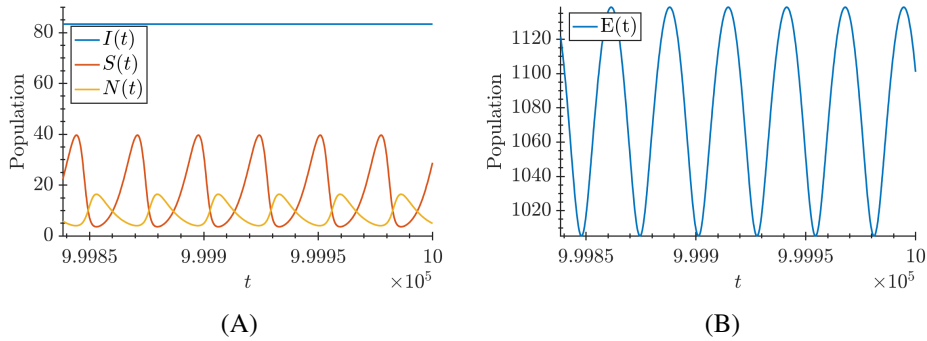


Figure 10: Time series data of the system also shows a clear picture of the oscillatory behavior between the populations in the invasion model. The plots visualize the long-term behavior of the system by time series data for (A)  $I, N, S$ , and (B)  $E$  populations.

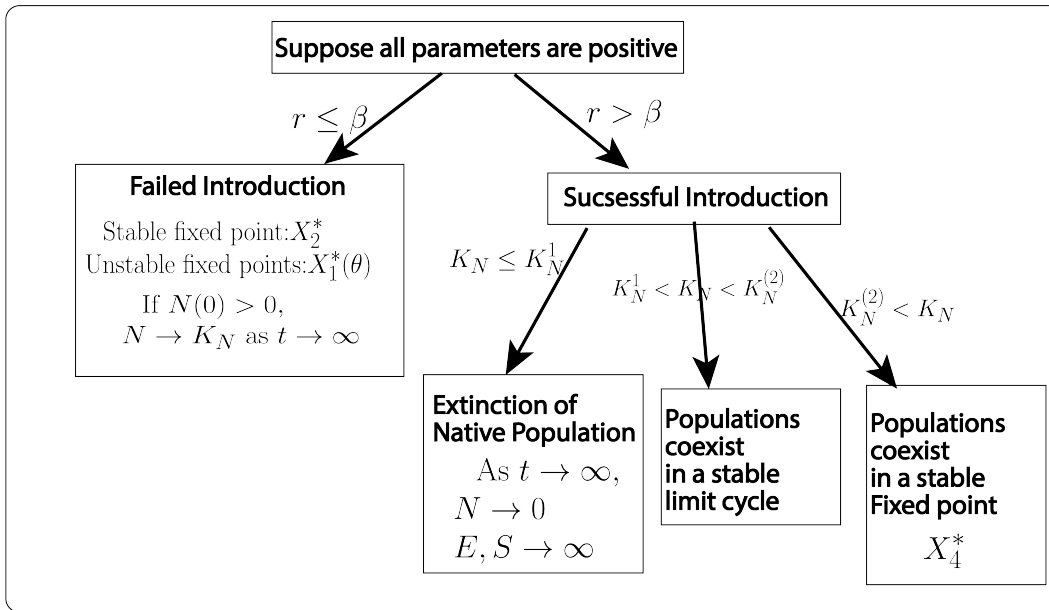


Figure 11: A summary of possible scenarios and outcomes of the mathematical model. The figure illustrates the requirements for a successful invasion of the invaders. First, a successful introduction must occur, and the growth rate ( $r$ ) should exceed the removal rate( $\beta$ ). Depending on the carrying capacity ( $K_N$ ) of the native population, three different scenarios can arise. If  $K_N$  is relatively low ( $K_N < K_N^*$ ), the native population will go extinct while the invaders experience exponential growth. However, if the carrying capacity is within a certain range, both invaders and native populations can coexist, either exhibiting periodic behavior or stabilizing in a fixed point, determined by the specific  $K_N$  values.

lem of infectious disease emergence. This model is inspired by other models of biological invasions, some composed of a series of steps that describe the introduction of an invading species to its establishment in a new setting [2, 9]. Using an analogous model imbued with mathematics and computational algorithms, we reveal that the invasion process includes several nonlinear interactions.

Among the intriguing aspects of our findings include the role that the maximum per-capita growth rate of invasive species at the introduction phase and carrying capacity of native species play in determining whether an invasion will succeed. In the emergence context, the “native species” concept can mean many different things. In the case of a zoonotic pathogen, for example, the “native species” might refer to the microbes that exist within the host. This is especially relevant in the context of the microbiota, where microbial taxa co-exist in confined spaces, with limited resources [30]. In viral emergence contexts, the carrying capacity of native species may refer to existing viruses that infect a common cell type, or the activity of host immunity which limits the population of viruses [31].

These results have several important implications. For one, the disease emergence process should not be described in terms of overly simplistic steps with non-interacting elements, but rather, should utilize methods that can responsibly integrate actors and their dynamics. Relatedly, a complex systems approach can aid in our efforts to model, predict, and intervene in infectious disease emergence events and their downstream epidemiological consequences. Such dynamical perspectives may reveal fragilities in the disease emergence process that might be targeted for intervention. More generally, we must re-emphasize that the mathematical approaches here outlined were inspired by conceptual models from plant invasion. This is further support for the notion that purely ecological conceptions can be animated by mathematical approaches, and implores the need for continued dialogue between disparate fields (e.g., plant biology and mathematical epidemiology). Indeed, infectious disease emergence warrants a diversity of perspectives and tools that can better consider how the behaviors of actors, states, parcels of information and agents create the specter of emerging infectious diseases. In the future, we should consider other methods that can better capture nonlinearities that may exist in disease dynamics, Whether these be advanced mathematical methods, simulations, or machine learning approaches.

Code availability

Code can be found at <https://github.com/OgPlexus/complexinvasion1>

## Acknowledgements

The authors would like to thank the editorial board of the Northeast Journal of Complex Systems and two reviewers for very helpful comments on a prior draft of the manuscript. The authors would like to thank members of the Ogbunu and Moreno Labs for helpful discussions on various aspects of the project. CBO would like to thank the organizers of the workshop entitled “Evolution of Drug Resistance (2014)” at the Kavli Institute for Theoretical Physics at the University of California, Santa Barbara, where early aspects of the ideas in this workshop were first developed. CBO would like to thank the Clarkson Complex Systems Center for a seminar invitation, where aspects of this work were discussed. SAM was supported by a National Science Foundation (NSF) CAREER award (2045671) and a Burroughs Wellcome Investigator in the Pathogenesis of Infectious Disease (1021977). SS acknowledges support from the Seesel Postdoctoral Fellowship from Yale University. CBO acknowledges support the MLK Visiting Scholars and Professors Program from the Massachusetts Institute of Technology.

## References

- [1] Andersson, D. & Hughes, D. Antibiotic Resistance and Its Cost: Is It Possible to Reverse Resistance?. *Nature Reviews Microbiology*. **8**, 260-271 (2010), <https://doi.org/10.1038/nrmicro2319>
- [2] Divíšek, J., Chytrý, M., Beckage, B., Gotelli, N., Lososová, Z., Pyšek, P., Richardson, D. & Molofsky, J. Similarity of introduced plant species to native ones facilitates naturalization, but differences enhance invasion success. *Nature Communications*. **9**, 1-10 (2018)
- [3] Ceddia, M., Bardsley, N., Goodwin, R., Holloway, G., Nocella, G. & Stasi, A. A complex system perspective on the emergence and spread of infectious diseases: Integrating economic and ecological aspects. *Ecological Economics*. **90** pp. 124-131 (2013)
- [4] Epstein, J. & Axtell, R. Growing artificial societies: social science from the bottom up. (Brookings Institution Press,1996)
- [5] Stephens, P., Altizer, S., Smith, K., Alonso Aguirre, A., Brown, J., Budischak, S., Byers, J., Dallas, T., Jonathan Davies, T., Drake, J. & Others The macroecology of infectious diseases: A new perspective on global-scale drivers of pathogen distributions and impacts. *Ecology Letters*. **19**, 1159-1171 (2016)

- [6] Archie, E., Luikart, G. & Ezenwa, V. Infecting epidemiology with genetics: a new frontier in disease ecology. *Trends In Ecology & Evolution*. **24**, 21-30 (2009)
- [7] Bharti, N. Linking human behaviors and infectious diseases. *Proceedings Of The National Academy Of Sciences*. **118** (2021)
- [8] Scarpino, S. & Petri, G. On the predictability of infectious disease outbreaks. *Nature Communications*. **10**, 1-8 (2019)
- [9] Richardson, D. & Pyšek, P. Plant invasions: merging the concepts of species invasiveness and community invasibility. *Progress In Physical Geography*. **30**, 409-431 (2006)
- [10] Thakur, M., Putten, W., Cobben, M., Kleunen, M. & Geisen, S. Microbial invasions in terrestrial ecosystems. *Nature Reviews Microbiology*. **17**, 621-631 (2019)
- [11] Hurwitz, A. & Others On the conditions under which an equation has only roots with negative real parts. *Selected Papers On Mathematical Trends In Control Theory*. **65** pp. 273-284 (1964)
- [12] Balasubramanian, D., López-Pérez, M., Grant, T., Ogbunugafor, C. & Almagro-Moreno, S. Molecular mechanisms and drivers of pathogen emergence. *Trends In Microbiology*. (2022)
- [13] Visher, E., Evensen, C., Guth, S., Lai, E., Norfolk, M., Rozins, C., Sokolov, N., Sui, M. & Boots, M. The three Ts of virulence evolution during zoonotic emergence. *Proceedings Of The Royal Society B*. **288**, 20210900 (2021)
- [14] Marshall, B. & Galea, S. Formalizing the role of agent-based modeling in causal inference and epidemiology. *American Journal Of Epidemiology*. **181**, 92-99 (2015)
- [15] Rutter, H., Savona, N., Glonti, K., Bibby, J., Cummins, S., Finegood, D., Greaves, F., Harper, L., Hawe, P., Moore, L. & Others The need for a complex systems model of evidence for public health. *The Lancet*. **390**, 2602-2604 (2017)
- [16] Sakai, A., Allendorf, F., Holt, J., Lodge, D., Molofsky, J., With, K., Baughman, S., Cabin, R., Cohen, J., Ellstrand, N. & Others The population biology of invasive species. *Annual Review Of Ecology And Systematics*. pp. 305-332 (2001)

- [17] Lavergne, S. & Molofsky, J. Reed canary grass (*Phalaris arundinacea*) as a biological model in the study of plant invasions. *Critical Reviews In Plant Sciences*. **23**, 415-429 (2004)
- [18] Hulme, P., Bacher, S., Kenis, M., Klotz, S., Kühn, I., Minchin, D., Nentwig, W., Olenin, S., Panov, V., Pergl, J. & Others Grasping at the routes of biological invasions: a framework for integrating pathways into policy. *Journal Of Applied Ecology*. **45**, 403-414 (2008)
- [19] Takahashi, L., Maidana, N., Ferreira, W., Pulino, P. & Yang, H. Mathematical models for the *Aedes aegypti* dispersal dynamics: travelling waves by wing and wind. *Bulletin Of Mathematical Biology*. **67**, 509-528 (2005)
- [20] Shampine, L. & Reichelt, M. The matlab ode suite. *SIAM Journal On Scientific Computing*. **18**, 1-22 (1997)
- [21] Dormand, J. & Prince, P. A family of embedded Runge-Kutta formulae. *Journal Of Computational And Applied Mathematics*. **6**, 19-26 (1980)
- [22] Schelling, T. Dynamic models of segregation. *Journal Of Mathematical Sociology*. **1**, 143-186 (1971)
- [23] Axelrod, R. The complexity of cooperation: Agent-based models of collaboration and competition. *Englewood Cliffs, NJ: Princeton University Press. Billings, SA And Coca, D.(2002) Identification Of Coupled Map Lattice Models Of Deterministic Distributed Parameter Systems. International Journal Of Systems Science*. **33**, 623-634 (1997)
- [24] Aleaga Aguilera, L. Preventing The Introduction And The Spread Of Freshwater Invasive Invertebrates In Ontario: Assessment Of The Proposed Invasive Species Act (bill 37). (2015)
- [25] Westphal, M., Browne, M., MacKinnon, K. & Noble, I. The link between international trade and the global distribution of invasive alien species. *Biological Invasions*. **10** pp. 391-398 (2008)
- [26] Dhooge, A., Govaerts, W., Kuznetsov, Y., Meijer, H. & Sautois, B. New features of the software MatCont for bifurcation analysis of dynamical systems. *Mathematical And Computer Modelling Of Dynamical Systems*. **14**, 147-175 (2008)
- [27] Hulme, P., Baker, R., Freckleton, R., Hails, R., Hartley, M., Harwood, J., Marion, G., Smith, G. & Williamson, M. The Epidemiological Framework for

Biological Invasions (EFBI): an interdisciplinary foundation for the assessment of biosecurity threats. (Pensoft Publishers,2020)

- [28] Ventura, P., Moreno, Y. & Rodrigues, F. Role of time scale in the spreading of asymmetrically interacting diseases. *Physical Review Research*. **3**, 013146 (2021)
- [29] Rutter, H., Savona, N., Glonti, K., Bibby, J., Cummins, S., Finegood, D., Greaves, F., Harper, L., Hawe, P., Moore, L. & Others The need for a complex systems model of evidence for public health. *The Lancet*. **390**, 2602-2604 (2017)
- [30] Senay, Y., John, G., Knutie, S. & Ogbunugafor, C. Deconstructing higher-order interactions in the microbiota: A theoretical examination. *BioRxiv*. pp. 647156 (2019)
- [31] Holland, J. & Domingo, E. Origin and evolution of viruses. *Virus Genes*. **16** pp. 13-21 (1998)
- [32] Haragus, M. & Iooss, G. Bifurcation Theory. *Encyclopedia Of Mathematical Physics*. pp. 275-281 (2006)
- [33] Françoise, J. Bifurcations of Periodic Orbits. *Encyclopedia Of Mathematical Physics*. pp. 285-290 (2006)
- [34] Kielhöfer, H. Bifurcation Theory: An Introduction with Applications to Partial Differential Equations. (Springer New York,2014)
- [35] Marsden, J. & McCracken, M. The Hopf bifurcation and its applications. (Springer Science & Business Media,2012)
- [36] Liebscher, S. Poincaré-Andronov-Hopf Bifurcation. *Bifurcation Without Parameters*. pp. 35-41 (2015)
- [37] Heppenstall, A., Crooks, A., See, L. & Batty, M. Agent-based models of geographical systems. (Springer Science Business Media,2011)
- [38] Railsback, S. & Grimm, V. Agent-based and individual-based modeling: a practical introduction. (Princeton university press,2019)



## Supplemental Material

### A ODE system

This section helps to visualize the stability analysis of the system of ODEs provided in the main article. Note that the Jacobian matrix at fixed point  $X^* = (I^*, E^*, S^*, N^*)$  is given by,

$$J(X^*) = \begin{bmatrix} r \left(1 - \frac{2I^*}{K_I}\right) - \beta & 0 & 0 & 0 \\ p\beta & \frac{-\alpha a}{a+N^*} & \gamma & \frac{a\alpha E^*}{(a+N^*)^2} \\ 0 & \frac{\alpha a}{a+N^*} & -(c_1 N^* + \gamma) & -c_1 S^* - \frac{a\alpha E^*}{(a+N^*)^2} \\ 0 & \frac{-c_3 b N^*}{K_N} & \frac{-c_2 b N^*}{K_N} & b \left(1 - \frac{2N^* + c_2 S^* + c_3 E^*}{K_N}\right) \end{bmatrix} \quad (10)$$

The characteristic polynomial of  $J(X^*)$  will reduce to the form in equation 5

$$\left( r \left(1 - \frac{2I^*}{K_I}\right) - \beta - \lambda \right) (\lambda^3 + B_2 \lambda^2 + B_1 \lambda + B_0) = 0$$

where,

$$\begin{aligned} B_2 &= D_1 + D_2 - D_3 \\ B_1 &= D_1 D_2 + D_7 D_9 + D_4 D_5 - (D_1 D_3 + D_2 D_3 + \gamma D_1) \\ B_0 &= D_2 D_7 D_9 + \gamma D_1 D_3 + D_1 D_4 D_5 - (D_1 D_2 D_3 + \gamma D_5 D_7 + D_1 D_4 D_9) \end{aligned} \quad (11)$$

with  $D_1 = \frac{\alpha a}{a+N^*}$ ,  $D_2 = (c_1 N^* + \gamma)$ ,  $D_3 = b \left(1 - \frac{2N^* + c_2 S^* + c_3 E^*}{K_N}\right)$ ,  $D_4 = \frac{-c_2 b N^*}{K_N}$ ,  $D_5 = c_1 S^* + \frac{a\alpha E^*}{(a+N^*)^2}$ ,  $D_6 = D_4 D_5$ ,  $D_7 = \frac{c_3 b N^*}{K_N}$ ,  $D_8 = D_5 D_7$ ,  $D_9 = \frac{a\alpha E^*}{(a+N^*)^2}$ , and  $D_{10} = D_1 D_4$ .

The dynamics of the introduction population can be found in figure (S2A). Figure (S1) demonstrate the sensitivity of the parameter  $K_N$ . The behavior of native, established, and spreading populations with no introduction population and non-zero native species is illustrated in figure S2B. The presence of a stable periodic orbit with a specific parameter set is further illustrated in figures S3A and S3.

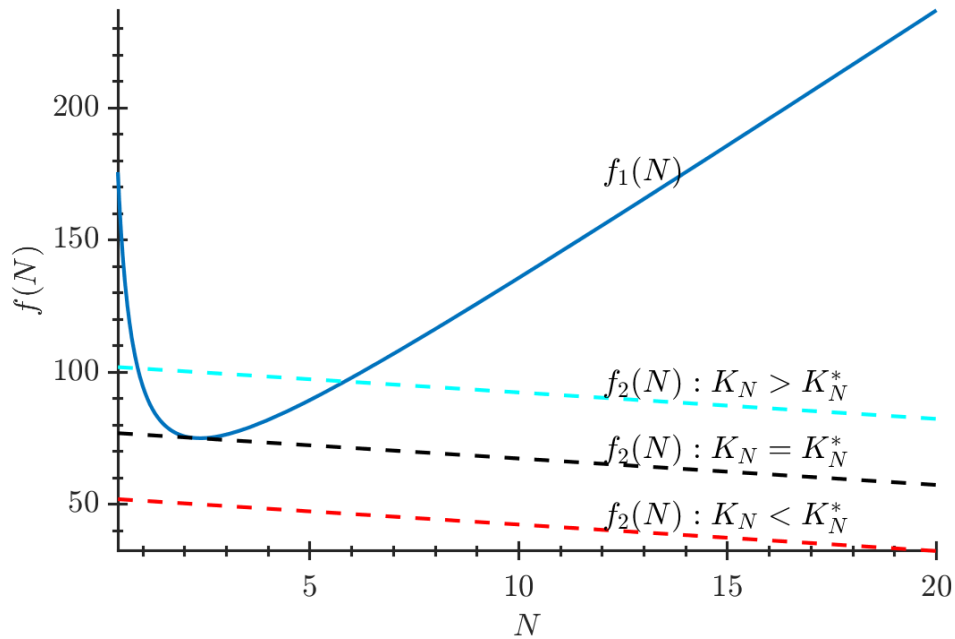


Figure S1: Figure demonstrates the critical  $K_N$  for the fixed point  $X_{3,4}^*$  scenario. In this figure,  $f_1(N) = C_2S^* + C_3E^*$  and  $f_2(N) = K_N - N$  where  $S^* = \frac{p\beta K_I(r-\beta)}{c_1rN}$  and  $E^* = \frac{p\beta K_I(r-\beta)(c_1N+\gamma)(a+N)}{a\alpha rc_1N}$ . Note that  $f_1$  and  $f_2$  can be derived by using  $F(X^*) = 0$ .

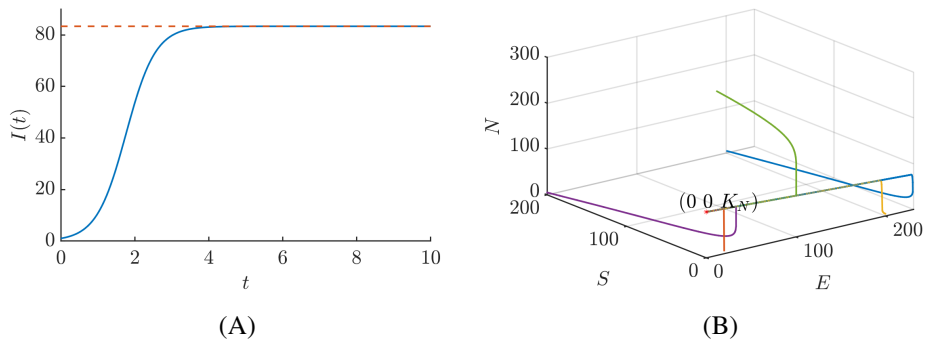


Figure S2: (A) Dynamics of the introduction population ( $I(t)$ ). Introduction population with non-zero initial condition (we used  $I(0) = 1$ ) will approach to the stable fixed point  $I_1^* = \frac{(r-\beta)K_I}{r}$  with the assumption  $r > \beta$ . (B) Dynamics of the native ( $N(t)$ ), established ( $E(t)$ ) and Spread ( $S(t)$ ) population with  $I(0) = 0$ . This figure demonstrates that each trajectory with  $(E(0), S(0), N(0) \neq 0)$  is approaching the fixed point  $(E^*, S^*, N^*) = (0, 0, K_N)$ .

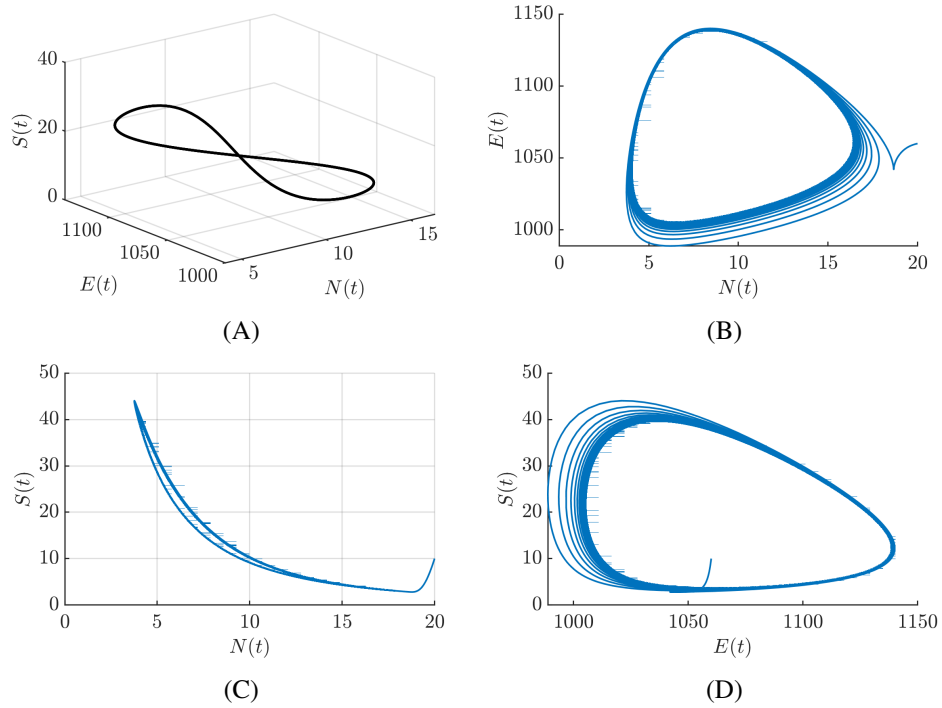


Figure S3: The ODE system with parameter values  $\Psi$  and  $K_N = 124$  approaches the stable periodic orbit shown in (A). Subsequent plots show the projection of  $X(t)$  with initial condition  $(1, 1060, 10, 20)$  to the (B)  $NE$ , (C)  $NS$  and (D)  $ES$  planes.

## B ABM System

### B.1 Agent based model

Here we offer an additional investigation of the dynamics of the system given a heterogeneous population *varying in fitness* among members of the invading species. We present an agent based model (ABM) [22, 23] iteration of the above ODE model. Similar to the ODE system, we continue to consider a single species invading through human-mediated dispersal in a homogeneous environment. However, the ABM model allows us to introduce a heterogeneous distribution of "fitnesses" among members of the invading agent (pathogen). This is in contrast to the homogeneous populations of single species invaders in the ODE system. Within the ABM each invader is considered an agent, and its stochastic movement among the four population groups is uniquely simulated. Due to fundamental differences between the ODEs and ABM approach, this variant of the system is not defined by a canonical set of equations. The ABM is implemented entirely in code (via Cython 0.29.13).

ABM facilitates the representation of a heterogeneous distribution by considering the behavior of individual agents of each population group [37, 38]. In this work, the inclusion of the command "shuffle(action list);" in the algorithm (Algorithm 3) ensures the performance of individualized actions in each time step. Specifically, the ABM implementation in Version 4 of the code in the notebook, under the corresponding section, allows for modeling a heterogeneous population distribution. This is achieved through lines 150 to 205 in code block 9, which introduce functionality that enables the model to iterate over diverse agent populations with distinct "fitness values." These fitness values, represented as unsigned floats, act as weights that scale the agents' capacity to transition between states in accordance with their movement through the state space of the model. It is worth noting that in the case of a homogeneous population, the fitness values would be uniform across all agents. However, heterogeneity emerges when the population consists of agents with varying fitness values. By incorporating this approach in the code, the concept of heterogeneity is effectively acknowledged and modeled by considering diverse fitness values within the agent population.

The ABM is initialized by defining a set number of individual agents of each population type,  $I_{Initial} = 84$ ,  $E_{Initial} = 100$ ,  $S_{Initial} = 0$ ,  $N_{Initial} = 190$ . Within the ABM the same set of four population types, the same directionality of population flow, as well as the same set of parameter types are maintained *as in* the ODE system. However, the terms guiding the agent's movements between each population type are no longer rate terms to be integrated over, but probabilities weighted by the model parameters. Following this, in the ABM case each parameter term is

a probability in units of *likely-hood/time step*. Each agent then moves between population types stochastically based on these probabilities. Additionally, unlike in the ODEs case each individual agent's movement is tracked independently (key algorithms 1 to 3, and functions used in the simulation can be found in the appendix). We recapitulate both the steady state and periodic orbit of the homogeneous ODE system. In order to do this we set the fitness of all members of the single invader equal, as in the ODEs case (see the Supplemental Informaton, figures S4 to S6 and section B) for further details).

## B.2 ABM Algorithm

To provide a better understanding of some of the key algorithms and functions used within this system, below is pseudo-code(see algorithms 1 to 3) that provides an overview of some fundamental operations and portions of the code comprising the model.

---

**Algorithm 1:** Here we provide a course grain outline of the primary ABM simulation loop. Each run is looped over then averaged, per run a set amount of time steps are executed wherein an action function is called for each time step for each agent.

---

**Data:** Number of runs, Number of time steps

---

```

begin
  foreach run; averaged do
    foreach time_step do
      action_list == sum( $\forall$  all_agents  $\in$  all_populations);
      shuffle(action_list);
      foreach agent  $\in$  action_list do
        agent_found = find_which_population_type(agent) ;
        action_function(agent_found);
        export: each agent_state per time step;
      end
      export: each agent_state per run;
    end
  end

```

---

## B.3 Supplemental figures for ABM

When the ABM has homogeneous agents then the system dynamics of the ABM should demonstrate the same dynamics to the ODE model. Figures (S5) and (S5)

---

**Algorithm 2:** Here we provide a course grain outline of the primary *find\_which\_population\_type* function referenced in Algorithm 1

---

```

Def - Find_Which_Population_Type (agent):
begin
  | if agent ∈ X_population
  |   return ('X')
end

```

---



---

**Algorithm 3:** Here we provide a course grain outline of the primary *action\_function* function referenced in Algorithm 1

---

```

Def - Action_Function (agent_found):
begin
  | if agent_found ∈ I_population
  |   | if param_prob == True
  |   |   move : agent_found
  |   elif agent_found ∈ E_population
  |   |   | if param_prob == True
  |   |   |   move : agent_found
  |   elif agent_found ∈ S_population
  |   |   | if param_prob == True
  |   |   |   move : agent_found
  |   elif agent_found ∈ N_population
  |   |   | if param_prob == True
  |   |   |   move : agent_found
end

```

---

illustrate the system dynamics of ABM with the same fitness across all agents which agreed with our results from ODE model.

Figure (S6) presents the system dynamics while varying fitness across the agents within the model. We also experiment with the effects of varying fitness (as defined above) on the populations of invading agents within each state as the model moves forward in time. Notably, as fitness is increased the number of invading agents within the established (*E*) population forms a peak near ~50 days before sharply decreasing, only to later rebound at ~200 days (the ~ notation indicate an estimate or approximation). This initial peak is a local/false maxima. The native (*N*) population shows an initial (0 - ~75 days) rapid increase before ever-more quickly declining, as the invading agent's fitness is increased. Inversely, the *S* population appears to only increase in the later stages of the model (~50 - ~200) days as fitness

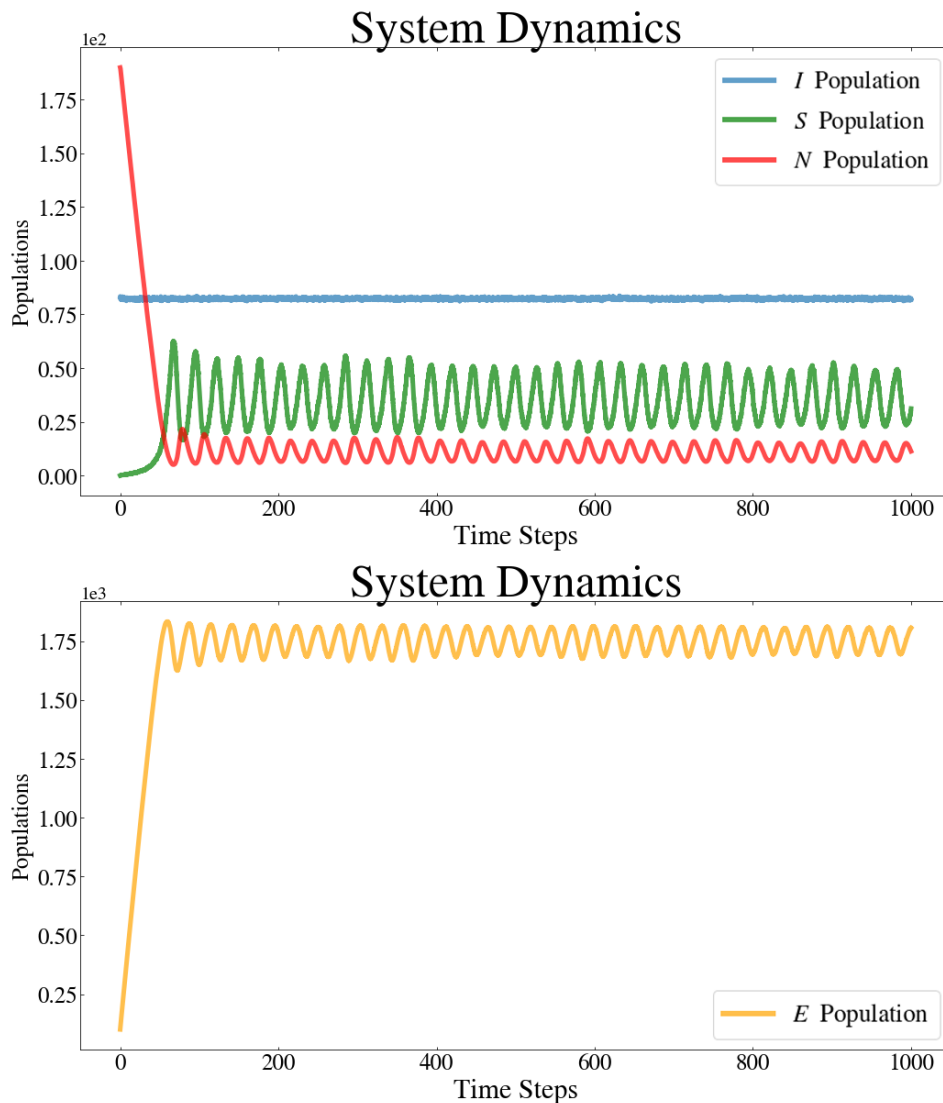


Figure S4: The figure shows the time-series evolution of the ABM system, which has similar behavior to the ODE system around  $K_N = 124$ .

is increased. As fitness increases the *I* population shows a rapid decline in the early stages (0 - ~50) days of the model before increasing again after ~75 days. This is similar to the behavior of the *E* population, however as fitness is increased the *I* population becomes more uniform after this initial ~50 day period.

To summarize, within the ABM as fitness increases we can see a greater number of invading agents establish in the system initially (0 - ~75) days, however this establishment is short lived (on the order of ~20 days) and represents only a local/false

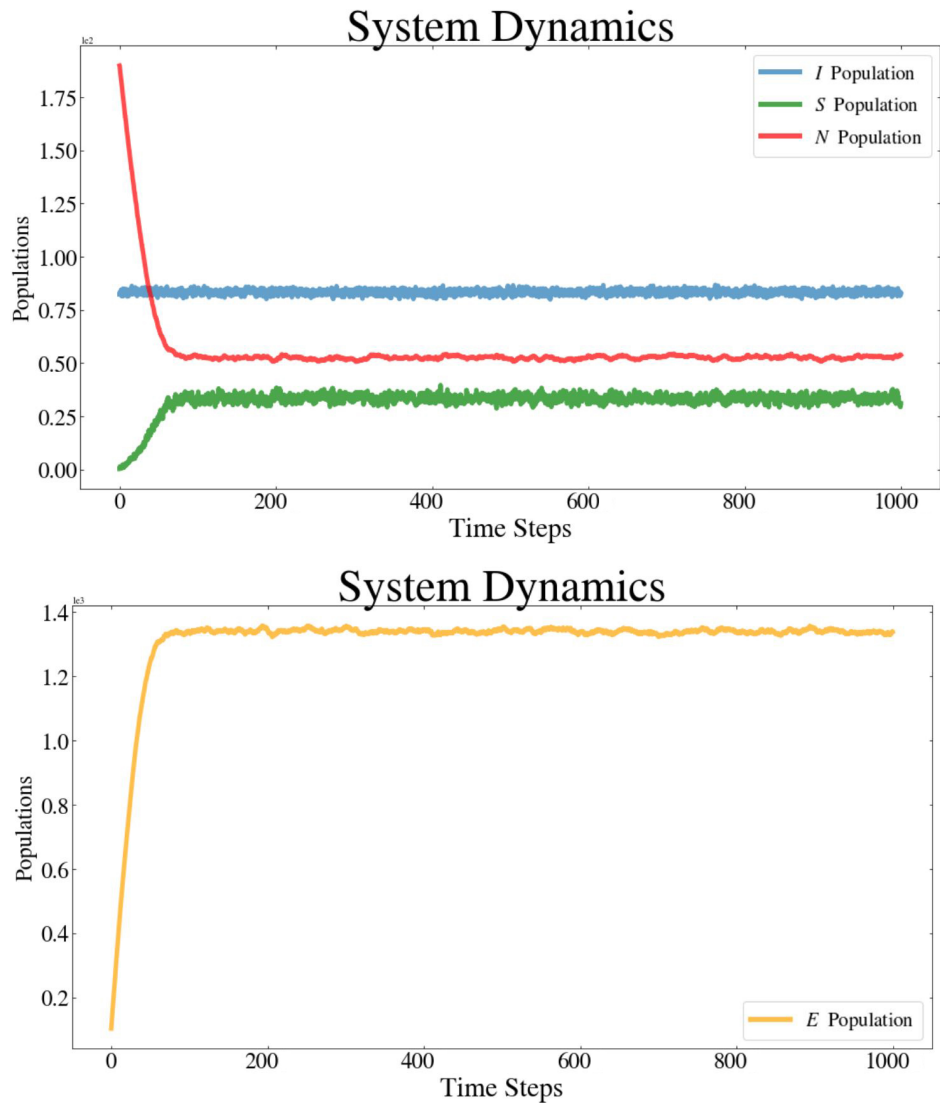


Figure S5: The figure shows the time-series evolution of the ABM system, which has similar behavior to the ODE system when  $K_N > 126$ .

maxima. After ( $\sim 75$ ) days a sharp decline occurs in the established invading population. Then it is only in the later stages of the model,  $\sim 150+$  days, that the invading agents are able to "regain ground" and establish once again with many reaching the final spread (S) state, between  $\sim 150 - \sim 300$  days. Additionally, we see that as invading fitness is increased the native population is more quickly (in  $\sim 25$  days at +90% fitness vs in  $\sim 100$  days at uniform fitness) destroyed by the invading agents during the initial early (0 -  $\sim 75$  days) establishment peak (local/false maxima).



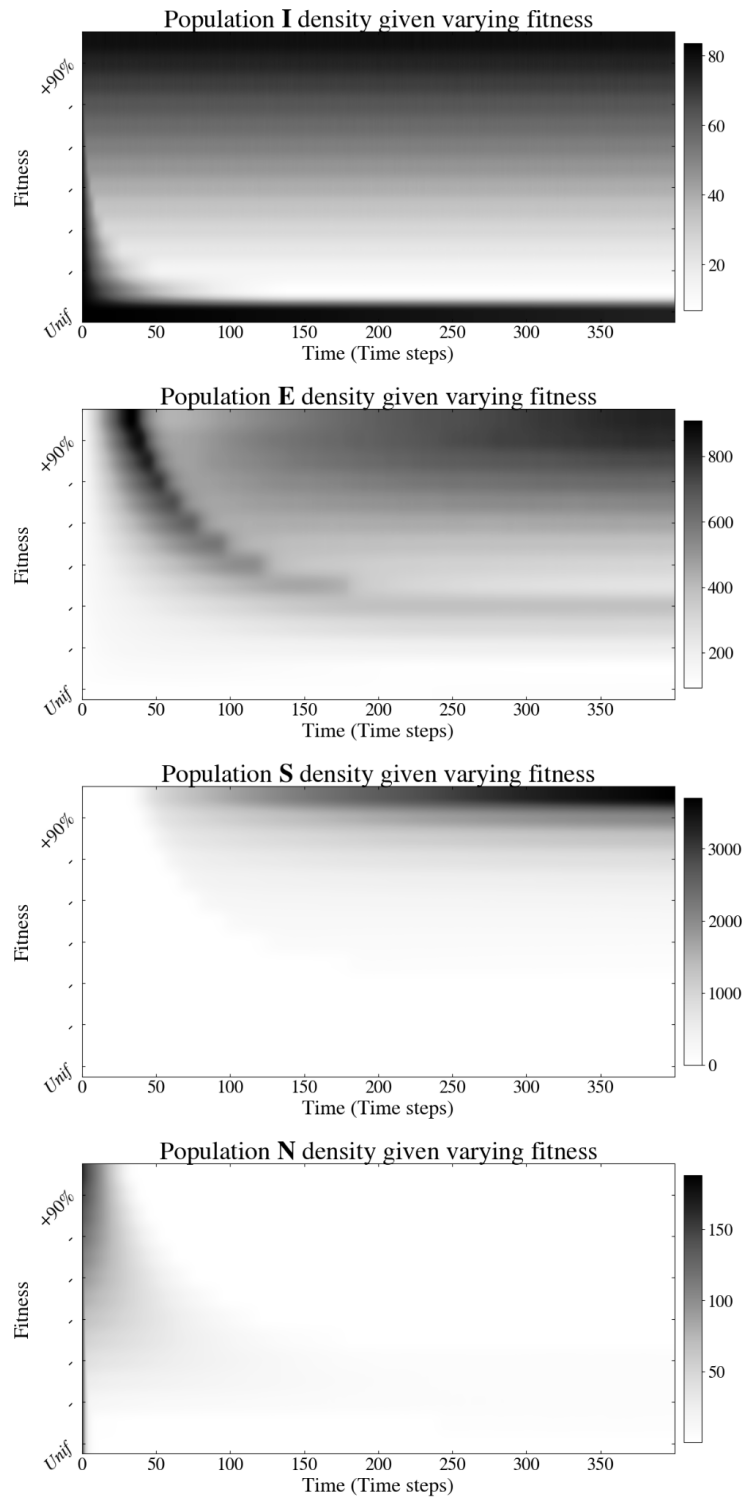


Figure S6: ABM time-series evolution of the number of agents within each state as fitness is varied within the model.